International Journal for Housing Science and Its Applications
Publish August 6, 2025. Volume 46, Issue 3 Pages 7316-7324

https://doi.org/10.70517/ijhsa463627

Quantitative computational analysis-based site-specific integrases in precision gene editing

Chang Wang[1,*]
[1] Chemical Engineering and Technology School of Tianjin University, Tianjin, 300072, China
Corresponding authors: (e-mail: veronica1104@163.com).

Abstract Site-specific integrases have shown great potential for application in the field of gene editing, making them promising to assist in the efficient and precise insertion of DNA fragments. In this paper, site-specific recombinases are used as an entry point to mediate recombination between sites using site-specific integrases. The formation and characteristics of the tyrosine recombinase family and the serine recombinase family are analyzed separately. Subsequently, the different structures and characteristics of the recognition sites on catalytic reactions of the two types of recombinase families are highlighted. Under this theoretical framework, pNZTS01 temperature-sensitive plasmid, pNZTS-PnisA-dCas9-pmCDA1-DBtsI empty plasmid and pNZTS-CRISPR-cDBE-DBtsI empty plasmid were constructed to establish the temperature-sensitive backbone plasmid. Meanwhile, suitable targets were selected to synthesize sgRNA expression cassettes and establish base editor plasmids, thus proposing a gene editing method based on site-specific recombinase. In the in vivo therapeutic effect observation experiment of RNA nanococoon in mice, RNCOs-D induced the highest tumor growth inhibition rate (~78%), which verified that the gene editing based on site-specific recombinase could effectively inhibit tumor growth.

Index Terms site-specific integrase, gene editing, base editor plasmid, temperature-sensitive backbone plasmid

I. Introduction

Gene editing technology has developed rapidly in recent years. The emergence of gene editing has made more precise gene regulation a reality, allowing a series of artificial modifications of genomic target as points through gene insertion, gene knockout and base substitution to obtain new functions or phenotypes [1]-[4]. In previous transgenic studies such as transgenic animal preparation, as well as gene therapy, viral vectors and randomized integration vectors have been mostly used for gene transfection [5], [6]. Although these vectors are effective in gene transfection, they face the deficiency that the target gene cannot be specifically integrated [7]. Although the later development of targeting vectors solved the problem of random integration of target genes to a certain extent, the targeting efficiency is not high in actual operation, and it increases the workload of researchers, which limits the application of targeting vectors and the development of transgenic technology to a large extent [8]-[10].

In recent years, site-specific recombinases with the characteristics of substrate specificity, fast and efficient, and easy to be modified for application have gained wide attention [11]. This enzyme can promote site-specific recombination between two DNA strands and achieve targeted and efficient integration without the need for external energy or cofactors [12], [13]. Its mediated recombination reactions are also widely used in genetic engineering operations [14].

In this paper, the formation, structure and properties of site-specific recombinase are firstly described in detail, and the structure and conformation of the recombinase recognition site in the site-specific recombination system are further analyzed, which serve as the theoretical basis of this study. We designed a temperature-sensitive backbone plasmid construction process, and established a base editor plasmid through target design and sgRNA insertion. Secondly, take in vitro LR clonase as the research object, carry out the experiment of measuring the recombination efficiency of in vitro LR clonase, and construct the error-prone PCR reaction system. Finally, we combined qualitative and quantitative methods to test the biocompatibility of RNA nanocococoon and the anti-tumor therapeutic effect in vivo.

II. Gene editing based on site-specific recombinases

II. A. Site-specific recombinases

There are two main categories depending on the method of vector used for transgenesis: viral vector-mediated gene transfer techniques and non-viral transgenic systems. The latter, also known as synthetic vector systems,

consist mainly of transfection reagents that can mimic the function of a viral capsid and one or more non-viral plasmid vectors that encode the target gene and enzymes that may be involved in assisted integration. In general, the success of gene transfer depends on the efficiency of mediating the entry of the target gene into the target cell, yet there are barriers from both the extracellular and intracellular environments in mediating the route of entry of the target gene into the cell.

Viral vectors, which can mediate efficient gene transfer, are mainly retroviral vectors and adenoviral vectors (AdV). Adenovirus-associated viral vectors (AAV) are the smallest viral vectors, which are increasingly valued for their non-inflammatory and non-pathogenic properties. Although the ability of viral vectors to mediate efficient gene transfer has led to their widespread use in gene therapy, the use of viral vectors still has certain drawbacks, such as small vector loads, complex production and purification processes, and the possibility of causing inflammatory reactions leading to immunologic complications.

Overall, non-viral vector systems are less cytotoxic and immunogenic than viral transduction. However, the traditional randomized integration method is often accompanied by obvious drawbacks: it is unable to control the integration site and the number of integrated copies of the transferred genes, which leads to inconsistent expression levels of the transferred genes, and randomized integration also carries the risk of insertional mutagenesis. Insertion mutagenesis is a concern because if the insertion site occurs near an oncogene or a tumor suppressor gene, it may lead to cancer. These defects can be mitigated by the use of site-specific recombinases. In nature, site-specific recombinases are found mainly in bacteria and phages, with only small amounts in eukaryotes. The widespread use of site-specific recombinases is due to the fact that they are equally functional in organisms other than those in which they originated. Site-specific recombinases are divided into two main families according to their evolutionary history and integration mechanism, which are called the tyrosine recombinase family and the serine recombinase family based on the amino acid residues that catalyze the integration reaction.

The tyrosine recombinase family is found predominantly in prokaryotes, with a few specific families in archaea, fungi, ciliates, and reverse transcription transposons. The tyrosine recombinase family includes λ phage integrases, Cre dissociases, Flp convertases, and other tyrosine recombinases. In nature, λ integrases are involved in integration and excision reactions, Cre is generally involved in excision reactions, and Flp drives chromosome inversions. Today, the functions of these tyrosine recombinases are more widely used. Although these tyrosine recombinases can mediate site-specific recombination, the fact that the target site recognized after recombination is the same as before recombination results in tyrosine recombinase-mediated recombination reactions being a dynamic, reversible process, and the fact that some of the recombinases (e.g., λ integrases) require cofactors in order to mediate recombination reactions makes tyrosine recombinases particularly unsuitable for being the enzymes that mediate the stabilization of DNA integration.

Serine recombinases, which differ from tyrosine recombinases in both amino acid length (180 - 800 amino acids) and structural domain composition. Serine recombinase family members include $\gamma\delta$ and Tn3 dissociation enzymes from the mycobacterial bacteriophage Bxb1, and phiC31 integrase from $\phi C31$ of Streptomyces phage. This family establishes a covalent bond between the recombinase and the DNA target sequence it recognizes via a serine residue on the conserved N-terminal catalytic structural domain, followed by strand exchange via a hydroxyl group (-OH) on the catalytic serine. Site-specific unidirectional recombination occurs at the intersection between the phage attachment site (attP) and the bacterial attachment site (attB), resulting in the formation of two new heterodimeric sequences $attL$ and $attR$. Within this group, most serine integrase-mediated recombination reactions do not require cofactors, which allows serine integrases to be widely used on organisms other than the species of origin. In addition, serine integrase-mediated integration reactions are unidirectional and irreversible. These properties make serine integrases more attractive for site-specific integration applications.

II. B.Structure and conformation of the recognition site

Although the mechanisms by which the two classes of recombinant enzymes catalyze their reactions are significantly different, the sites at which they catalyze their reactions show no clear distinction and show little regularity, except for the fact that they all have short sequences of homologous regions at their cores. Some recognition sites are relatively complex, containing core sequences (chain exchange regions), protein-binding sequences, host cofactor-binding sequences, and so on. Others are very simple, requiring only a bipartite inverted repeat sequence separated by a spacer of a few tens of nucleotides.

The structures of the recognition sites of the site-specific recombinases are shown in Fig. 1. where (A) the $attP$ and $attB$ sites of E. coli phage λ contain homologous sequences of seven nucleotides, C, C', B and B' are inverted repeats, and P1, P2, P'1, P'2, and P'3 are Int-binding sites, with three Xis (cleavage disassembly enzyme) binding sites, one Fis binding site and three IHF binding sites (H1, H2, H'), (B) the recognition site of the P1 phage recombinase Cre is the 34 bp reverse-repeat sequence loxP, (C) the structure of the res site of the transposon

$\gamma\delta$ dissociase, (D) the Salmonella invertase Hin-mediated recombination system recognition site structure , (E) Schematic representation of the minimal integration substrate pair structure of Streptomyces phage ΦBT1.

The E. coli phage $\lambda-$ integrase recognizes its own attP site and the attB site in the E. coli chromosome, with the attP site being structurally complex and the latter relatively simple. Both the $attP$ and $attB$ sites contain a 7 bp core sequence in the center, which is flanked by 7 bp reverse repeats called C and C', and B and B', respectively. attP sites are more structurally complex, and also include arm-binding sites called P1, P2, P'1, P'2, and P' 3, all of which bind to integrase Int during the reaction. In addition, three host factor (IHF) binding sites, H1, H2 and H', three cleavage enzyme (Xis) binding sites, and a cofactor (Fis) binding site are included. λ Integrase achieves precise control of the direction of the recombination reaction precisely by means of such a complex substrate structure. In comparison, the Cre - loxP system encoded by E. coli phage P1 and the Flp - frt system encoded by the yeast 2μ plasmid have a much simpler structure of recognition sites. In both systems, there are no sequences other than the 8 bp core sequence and the perfectly symmetrical inverted repeats of 13 bp on each side that can bind to the cofactor. Because there is only one pair of identical recombination sites, the Cre - loxP and Flp - frt recombination systems are not tightly directionally controlled, and the reactions do not tend in one direction or another, but rather tend to equilibrate. It is generally accepted that tyrosine recombinase systems require very strict homology of the DNA sequence of the core site. In the case of the λ system, for example, when the core sequence of one site is mutated, the reaction cannot proceed. When the same mutation is made in the core of another site, the reaction resumes. This is because the cut end of the core sequence is responsible for homologous pairing during single-stranded cleavage invasion. However, the core region of the recognition sequence of the integrase encoded by Enterococcus faecalis transposon Tn916 and Streptococcus pneumoniae transposon Tn1545 is not homologous. Recent studies have found that the CtnDOT recognition site characterization of transposon CtnDOT of the genus Anaplasma is consistent with Tn916 and Tn1545, and that after recombination the core site bases are not paired and need to undergo further replication to remain genetically stable. The homology requirement of transposon NBU1 for the recognition site is not at the recombination site. In contrast, phage CTX achieves recombination with non-homologous core sites through a single-strand exchange mechanism. This all challenges the traditional model of homologous end invasion to form Holliday Junction intermediates.

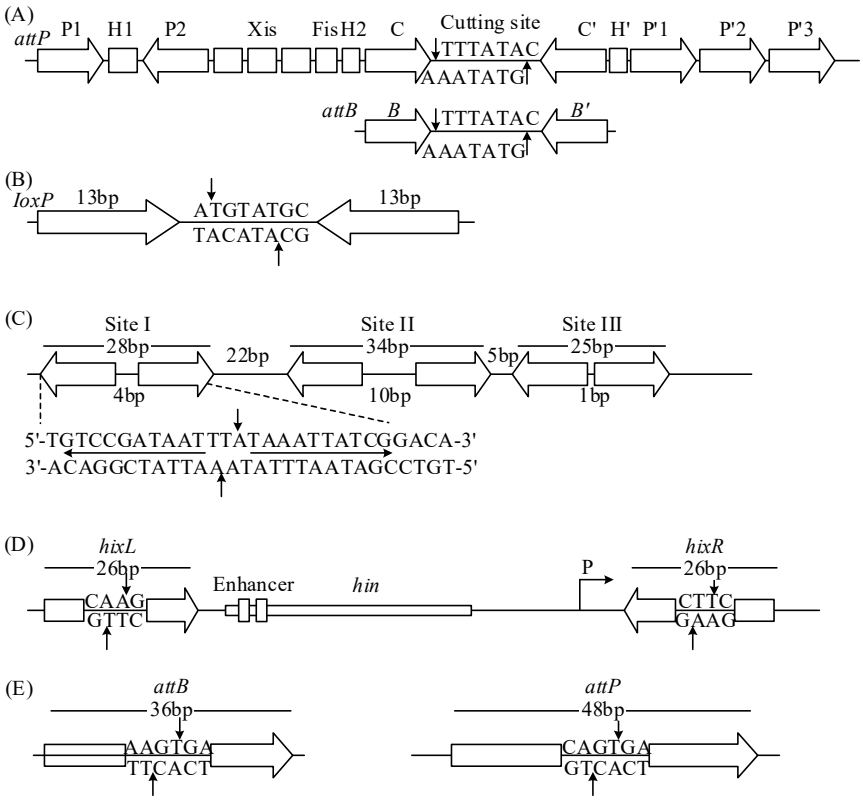

Figure 1: The recognition site structure of site-specific recombinase

The res site of serine dissociation enzyme $\gamma\delta$ is nearly 120 bp and contains 3 dimeric protein binding sites siteI, siteII and siteIII. The cleavage site is located at siteI, but the other 2 sites are also required for recombination. The spatial position of the three sites is very important.The three sites are characterized as rare in dimer binding and each has a different geometrical conformation. All contain a pair of tail-to-tail recognition sequences, but the spacer sequences of the three sites differ in length, being 4, 10 and 1 bp, respectively. As a side note, the unusual flexibility of the $\gamma\delta$ dissociase dimer (also seen in other serine recombinases) allows the DNA-binding domain to adapt to different spacings and conformations. The accessory sites SiteII and SiteIII are particularly important for controlling the outcome of the reaction. The recognition sequence for the invertase Hin is a 26 bp two-segment inverted repeat sequence, hinL and hinR, with the hin gene lying between the two sites. Hin mediates promoter inversion to control downstream gene expression. The reaction requires the participation of Fis, whose recognition site is an enhancer containing two dimeric recognition sequences separated by 48 bp. The recognition site of phage-encoded large serine recombinases is relatively simple. Taking the $\phi BT1$ integrative system as an example, except for its core region containing 9 bp of homologous sequences, the two sites are significantly different, but all have 5'-GT as the core and show irregular inverted repeats, and the minimum recognition sequences are 36 (attB) and 48 bp (attP), respectively.

The mechanism of action of site-specific recombinases is similar to that of topoisomerases, so it is generally accepted that the recombination process requires a substrate conformation. In the Hin inversion process, the pairing of substrates and the formation of the inversion complex are separated, and a low degree of negative superhelix is sufficient to initiate pairing, but a high degree of negative superhelix is required for the formation of the inversion complex. Linker substrates that do not possess a superhelix can also complete association in the presence of Tn3 dissociative enzymes, but superhelix is required for the postassociation process. In $\gamma\delta$ dissociation, the reaction efficiency of the missing linker substrate is about 50% of that of the superhelix. As long as the two sites are located on the superhelical loop, Gin invertase can utilize the enhancer located on the notched loop to complete the reaction. In the Xer system, cer sites under different degrees of negative superhelix were able to recombine, but the recombination efficiency of the mwr site decreased significantly with the weakening of the degree of helix. However, in vitro studies of integrative systems such as phage λ, $\phi C31$, $\phi BT1$, $Bxb1$, $\phi Rv1$, etc., have found that recombination of the linear substrate occurs efficiently as long as there is a suitable buffer system and that there is no requirement at all for a superhelicoidal state of the substrate, although integrases still mediate superhelical relaxation of the substrate.

II. C.Temperature-sensitive backbone plasmid and base editor plasmid construction

(1) pNZTS01 temperature-sensitive plasmid construction: pNZTS01 plasmid mainly consists of two parts, one part is pWV01ts-Ery resistance gene, which is a part of the DNA fragment obtained by PCR amplification and purification and recovery of the target strips using the primer TSOri-F/R with pNZts-Cre as the template, and UC57ori is the E. coli high-copy replicon. The UCori-F/R primers were obtained by PCR amplification and recovery by purification using the pUC57 vector as a template, followed by assembly of the two fragments using seamless cloning. The amplification and purification of the target fragments, the assembly of seamless clones of single fragments, and colony PCR were performed as described previously and will not be repeated.

(2) pNZTS-PnisA-dCas9-pmCDA1-DBtsI empty plasmid construction: using linearized primer LpNZts-F/R to amplify with pNZTS01 as the template, and after amplification, the plasmid template was digested using $Dpn\,I$, and finally purified and recovered by cutting the gel. Linker-pmCDA1 fragment was synthesized by Jin Weizhi. The Linker-pmCDA1 fragment was synthesized by JinWeiZhi, and the plasmid provided by JinWeiZhi was used as the template to amplify the target bands using the primers dpmCDA-F/pmCDA-R and purified and recovered. P_{nisA} promoter was amplified in pNZ8148 vector and dCas9 was amplified in pLEB-dCas9 vector, and after both were purified and recovered, overlapping PCR was carried out using the primers dPnisA-F/dCas9-R, and the target fragments PnisA-dCas9 were purified and recovered at last. Assembly Master Mix to seamlessly clone PnisA-dCas9 and Linker-pmCDA onto the linearized pNZTS01 plasmid.

(3) pNZTS-CRISPR-cDBE-DBtsI empty plasmid construction: pNZTS-PnisA-dCas9-pmCDA1 plasmid was used as a template, and primer XLUGI-F/dPnisA-R amplified the plasmid backbone. The dCas9-Linker fragment was amplified using the dCas9-F/XLdCas-R primer, and the Linker-F/R primer amplified a 363 bp Linker. Primers UGI-F/R, UGI-1, 2, and 3 were used to synthesize UGILVA. After purification and recovery, the fragments pmCDA1, linker, and UGILVA were overlapped and purified and recovered using primers Linker-F/UGI-R. Finally, the plasmid backbone and the three fragments dCas9-Linker, pmCDA1-Linker-UGILVA were seamlessly cloned using NEBuilder® HiFi DNA Assembly Master Mix. The specific experimental methods for amplification and purification of target fragments and seamless cloning assembly of single fragments, colony PCR, etc. were described previously and will not be repeated.

(4) Target design and sgRNA insertion: The design and selection of gRNA targets are related to the success of base editing, and it is found that most of the gene editing windows of vectors constructed with Cas9 variants and pmCDA1 are -20 to -16, so the bioinformatics software CRISPR-offfinder is used to design the targets, and the targets with multiple C bases and high scores at the -20 to -16 positions are selected for subsequent verification as much as possible. To determine the activity window of the base editor in Lactococcus lactis, three Cs were specifically screened for targets whose positions could completely cover the -20 to -1 positions. After selecting suitable targets, 71 nt primers were synthesized and combined with three universal primers for template-free PCR to synthesize the sgRNA expression cassette. The target fragments were purified and recovered, and then ligated into the plasmid backbone using EasyFusion Assembly Master Mix, which was linearized using the $Bts\ I$ -enzyme digestion. The specific experimental methods for amplification, purification and seamless clone assembly of the target fragment and colony PCR validation of the single fragment were described previously and will not be repeated.

III. Measurement of site-specific integrase and assessment of treatment efficacy

III. A. Determination of the recombination rate of LR clonase in vitro

The pMF.LA plasmid was extracted for LR recombination reaction in vitro. The parental plasmids of three standards (T-MP, T-MC and MF-PP) were diluted step by step and then subjected to fluorescence quantitative PCR reaction: the results of absolute quantitative PCR at different times of induction 2h, 4h, 6h, 8h and 10h are shown in Fig. 2. The recombination efficiency of the LR recombination reaction firstly increases and then decreases with the prolongation of time, and it reaches the highest value of 90% at 6h. With the extension of induction time, the proportion of parental plasmid was getting lower and lower, and the proportion of microplasmid/microcycle was getting larger and larger with the extension of induction time due to the ability of microplasmid to replicate autonomously.

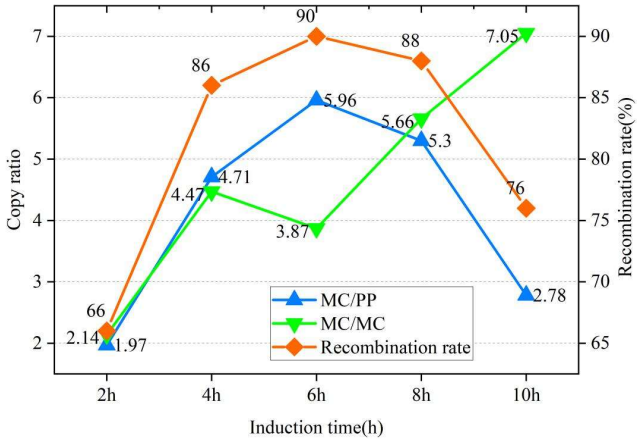

Figure 2: The relationship between in vivo LR recombination rate and time of pMF.LA

III. B. Determination of the recombination rate of LR clonase in vitro

Two standards (T-MC and MF-PP) were diluted step by step and then subjected to fluorescence quantitative PCR reaction. The recombination efficiencies at different reaction times of 2h, 4h, 6h, 8h and 10h are shown in Fig. 3. The efficiency of LR recombination reaction tended to increase with the extension of time, but there was no regularity, with the highest value of 11.8% at 10h. With the extension of induction time, the recombination efficiency did not produce a large increase.

III. C. Error-prone PCR systems

The results of error-prone PCR of pW1, pW2, and pW3 plasmids with error-prone PCR Taq enzyme using primers VF2/VR are shown in Table 1. 95°C denaturation for 2 min45s and 65 cycles of amplification: denaturation at 95°C for 55 s, annealing at 50°C for 65 s, and extension at 75°C for 65 s. The results of error-prone PCR were shown in Table 1.

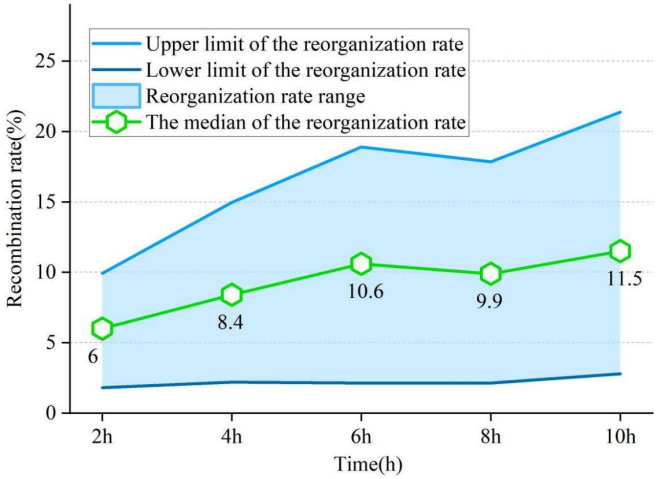

Figure 3: The relationship between in vitro LR recombination rate and time

Table 1: System of error prone PCR

Component	Volume(μL)
Plasmid(10 ng/μL)	2.5
VF2 (10 μmol/L)	3
VR(10 μmol/L)	3
Error-prone PCR Mix,10X	4.5
Error-prone PCR dedicated dNTP,10X	4.5
MnCl2, 5 mmol/L	4.5
Taq DNA polymerase	2
ddH2O	18
Total	42

III. D. In vivo therapeutic effects of RNA nanococoons

III. D. 1) RNA nanococoon biocompatibility

The mice were put to death 0, 5, 10 and 15 days after injection of RNCOs-D, and their blood samples were collected for hematological and blood biochemical analyses, and the organ damage and pathological changes are shown in Fig. 4. The results showed that the liver and kidney function indexes of mice treated with RNCOs-D were normal, and the routine blood tests also indicated that RNCOs-D exhibited non-toxic effects on Balb/c mice during the treatment period. The good biocompatibility of RNCOs-D in normal tissues was demonstrated, and it has great prospects for practical application.

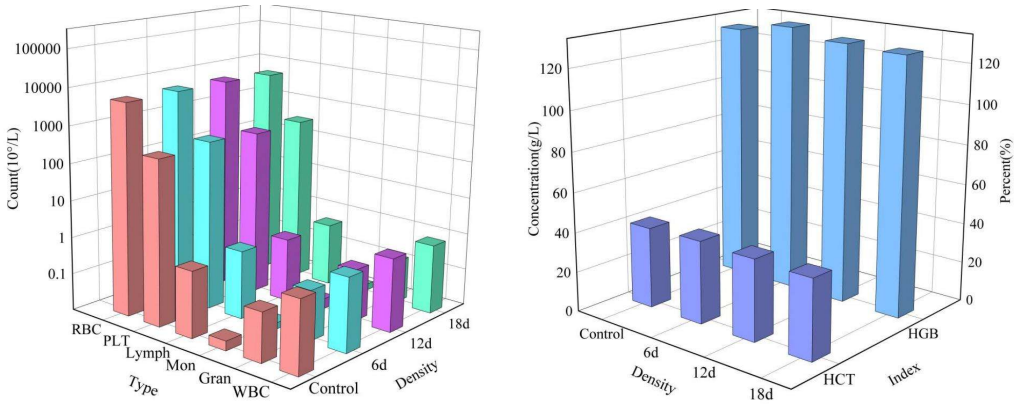

RBC, PLT, Lymph, Mon, Gran, WBC HCT, HGB

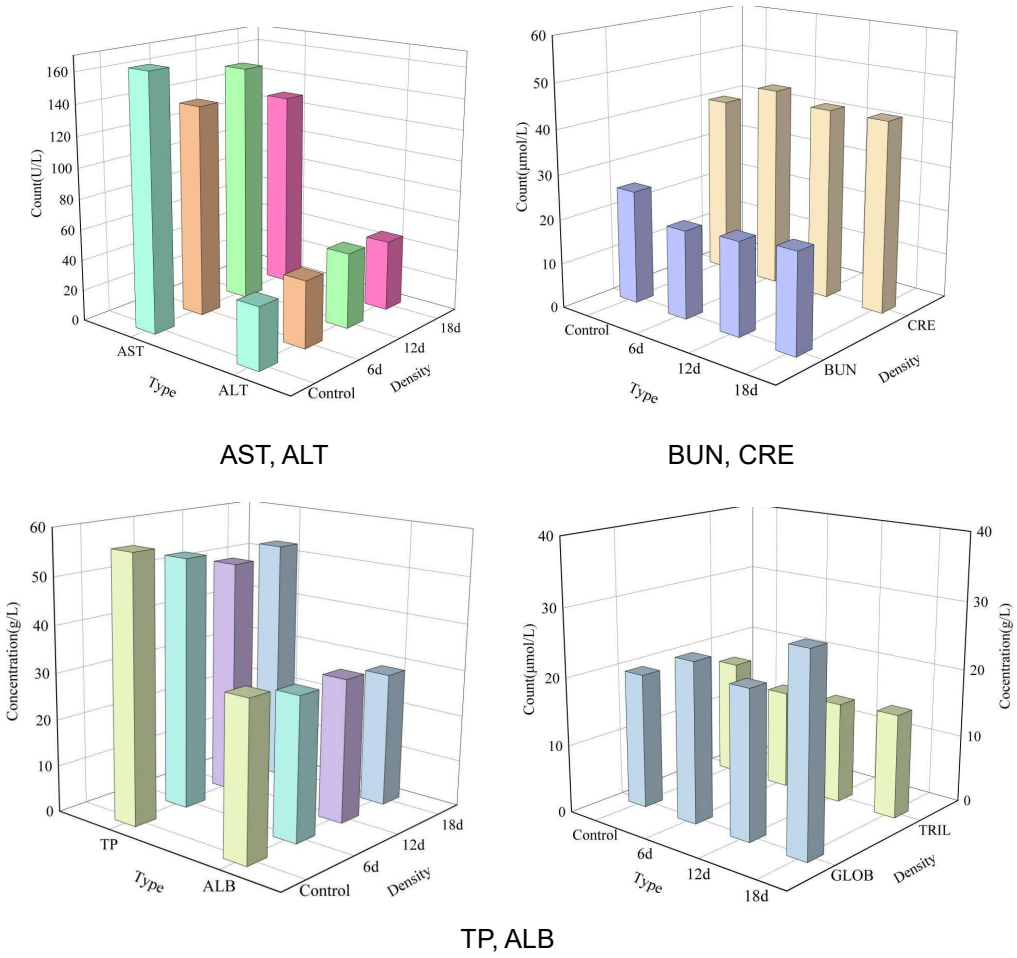

AST, ALT

BUN, CRE

TP, ALB

GLOB, TRIL

Figure 4: Organ damage and pathological changes in mice

III. D. 2) Anti-tumor effects of RNA nanococococoons in vivo

To test the in vivo therapeutic performance of RNCOs-D in the U87-EGFRvIII xenograft animal model, tumor-bearing mice were randomly divided into 6 groups (n=5 per group) and injected i.v. with PBS, DOX, rRNCOs-D, RNSs-D, nRNCOs-D, and RNCOs-D, respectively. During the 15-day treatment period, every 3 days, the mice's body weights and tumor volume. The body weight curves, tumor growth curves and tumor weights of mice treated with PBS, rRNCOs-D, RNs-D, nRNCOs-D and RNCOs-D are shown in FIGS. 5(a)-(c), respectively, and it can be found that mice treated with RNCOs-D have the smallest tumor size.

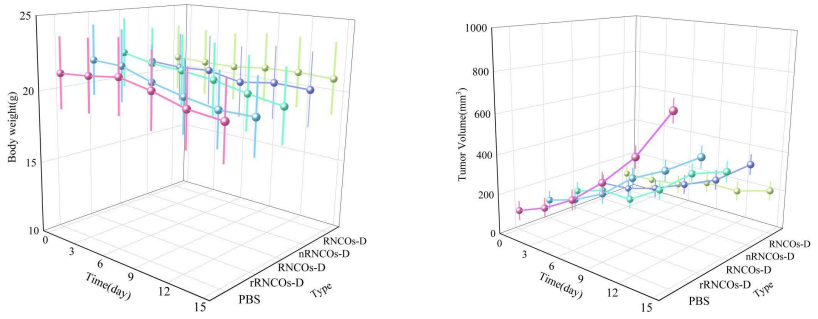

(a) Mouse body weight curve

(b) Tumor growth curve

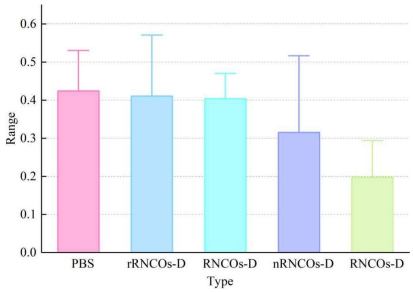

(c) Tumor weight

Figure 5: The changes in the body weight and tumor volume of mice

The tumor growth inhibition rates after treatment with PBS, rRNCOs-D, RNs-D, nRNCOs-D, and RNCOs-D are shown in Figure 6. RNCOs-D elicited the highest tumor growth inhibition rate (~78%), visually demonstrating that tumor growth can be significantly inhibited by synergistic gene/chemotherapy.

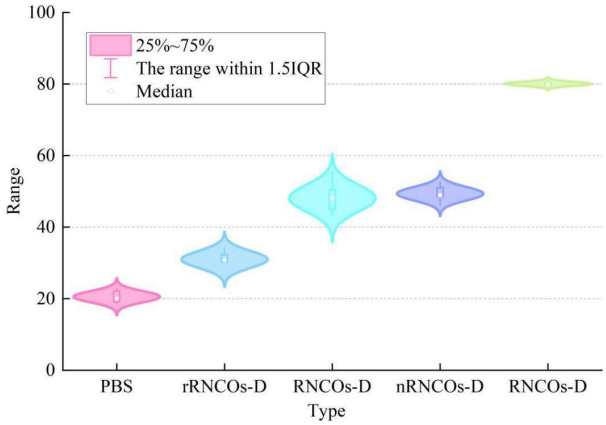

Figure 6: The growth inhibition rate after treatment

IV. Conclusion

In this paper, site-specific integrase combined with site-specific recombinase was utilized to construct temperature-sensitive backbone plasmids as well as base editor plasmids based on the recognition site characteristics of different classes of site-specific recombinases to realize the application of site-specific integrase in genetic engineering.

In the assay of site-specific integrase, the recombination efficiency of LR recombination reaction could reach the highest value of 90% at 6h in vivo, and it first increased and then decreased with the extension of time. In vitro, although it was able to reach a maximum value of 11.8% at 10h, there was no pattern. Further, in vivo experiments on the therapeutic effect of tumor treatment in mice were carried out using RNA nanococococoons, in which RNCOs-D had good biocompatibility in normal tissues and was able to induce the highest tumor growth inhibition (~78%), which verified that tumor growth could be significantly inhibited by synergistic gene/chemotherapy.

References

[1] Li, H., Yang, Y., Hong, W., Huang, M., Wu, M., & Zhao, X. (2020). Applications of genome editing technology in the targeted therapy of human diseases: mechanisms, advances and prospects. Signal transduction and targeted therapy, 5(1), 1.

[2] Yin, H., Kauffman, K. J., & Anderson, D. G. (2017). Delivery technologies for genome editing. Nature reviews Drug discovery, 16(6), 387-399.

[3] Wang, J. Y., & Doudna, J. A. (2023). CRISPR technology: A decade of genome editing is only the beginning. Science, 379(6629), eadd8643.

[4] Zheng, Y., Li, Y., Zhou, K., Li, T., VanDusen, N. J., & Hua, Y. (2024). Precise genome-editing in human diseases: mechanisms, strategies and applications. Signal Transduction and Targeted Therapy, 9(1), 47.

[5] Zu, H., & Gao, D. (2021). Non-viral vectors in gene therapy: recent development, challenges, and prospects. The AAPS journal, 23(4), 78.

[6] Khan, S. H. (2019). Genome-editing technologies: concept, pros, and cons of various genome-editing techniques and bioethical concerns for clinical application. Molecular therapy Nucleic acids, 16, 326-334.

[7] Chakrabarti, A. M., Henser-Brownhill, T., Monserrat, J., Poetsch, A. R., Luscombe, N. M., & Scaffidi, P. (2019). Target-specific precision of CRISPR-mediated genome editing. Molecular cell, 73(4), 699-713.
[8] Chen, P. J., & Liu, D. R. (2023). Prime editing for precise and highly versatile genome manipulation. Nature Reviews Genetics, 24(3), 161-177.
[9] van Haasteren, J., Li, J., Scheideler, O. J., Murthy, N., & Schaffer, D. V. (2020). The delivery challenge: fulfilling the promise of therapeutic genome editing. Nature biotechnology, 38(7), 845-855.
[10] Doudna, J. A. (2020). The promise and challenge of therapeutic genome editing. Nature, 578(7794), 229-236.
[11] Tian, X., & Zhou, B. (2021). Strategies for site-specific recombination with high efficiency and precise spatiotemporal resolution. Journal of Biological Chemistry, 296.
[12] Zhang, Z., Lu, Y., Chi, Z., Liu, G. L., Jiang, H., Hu, Z., & Chi, Z. M. (2019). Genome editing of different strains of Aureobasidium melanogenum using an efficient Cre/loxp site-specific recombination system. Fungal Biology, 123(10), 723-731.
[13] Bessen, J. L., Afeyan, L. K., Dančík, V., Koblan, L. W., Thompson, D. B., Leichner, C., ... & Liu, D. R. (2019). High-resolution specificity profiling and off-target prediction for site-specific DNA recombinases. Nature Communications, 10(1), 1937.
[14] Merkert, S., & Martin, U. (2018). Targeted gene editing in human pluripotent stem cells using site-specific nucleases. Engineering and Application of Pluripotent Stem Cells, 169-186.